

Geometric effects in the design of multijet impingement atomizers

M. R. O. Panão*, J. M. D. Delgado, A. L. N. Moreira

Instituto Superior Técnico, Technical University of Lisbon, Portugal

mpanao@dem.ist.utl.pt; joao.delgado@ist.utl.pt and moreira@dem.ist.utl.pt

Abstract

The multijet impingement atomization strategy stands out as competitive in the production of liquid atomizers with relatively simple geometries, producing sprays from the impingement of two or more jets ($N_j \geq 2$), with a relatively low injection pressure and, consequently, low flow rates ($< 1.5l/min$). However, there are two geometric factors affecting the design of these atomizers and, eventually, the atomization process itself, which are scarcely approached in the literature: i) the pre-impingement distance (l_{pi}) of the jets; ii) and the jets' misalignment. In this work, the impact of two cylindrical jets is considered. The analysis focus on the influence of these parameters in the structure of the liquid sheet formation, as well as drop size.

Introduction

The multijet impingement atomization strategy has been recently applied to a prototype having in mind the development of spray cooling concepts in microelectronics [1] and power electronic devices [2]. This strategy is described by the formation of a liquid sheet from the simultaneous impact of two, or more, cylindrical jets of a certain diameter (d_j). This liquid sheet further destabilizes and disintegrates into ligaments, and these fragment into droplets, thus forming the multijet impingement spray. In these previously mentioned works, the design of the atomizer was based on the knowledge reported in the literature for the atomization by the impact of two jets, particularly the works of Li and Ashgriz [3] and Bremond and Villermaux [4]. However, none of these works performs a systematic study on the effect of the pre-impingement distance of the jets, nor the possibility of jet misalignment, eventually occurring during the fabrication process. The study of these parameters is the motivation for the fundamental work presented here.

Most research works on two-impinging jets fix the pre-jet-impingement distance (l_{pi}). For example, in Shen and Poulikakos [5], $l_{pi}/d_j \approx 6.54$, while Bremond and Villermaux [4] fixed approximately at 3, Choo and Kang [6] at 10, and Li and Ashgriz [3] have fixed their experiments at 12.5. Therefore, the range of values used is quite sparse. Furthermore, these works considered laminar jets, and for turbulent jets, Panão et al. [1, 2] have used $l_{pi}/d_j = 6.8$, and Anderson et al. [7] reported that the free turbulent jet length had no apparent effect on spray formation. Jung et al. [8] have considered different free jet lengths, but in asymmetric fashion, i.e. the distance is changed in only one of the two jets, and their purpose was to study the influence of this asymmetry in the fishbone instability. Therefore, this shows the gap in the literature relatively to the effect of the pre-jet-impingement distance on the atomization process, toward which the present work intends to contribute with experimental evidence and mitigate this gap.

Moreover, relatively to the effect of jet misalignment, only in Gadgil and Raghunandam [9] can we find a systematic study, in the range of jet Reynolds number (Re_j) between 9000 and 30000. The obvious effect of jet misalignment is the rotation of the liquid sheet caused by the partial impact between the jets. In this case, the moment in the direction of jet propagation has a non-zero component, contrary to the aligned case. The effect was particularly evident in drop size, which decreases with the rotation angle. Given the high range of Re_j used in their experiments, no discernable effects could be observed relatively to the fundamental hydrodynamics associated with liquid sheet formation, disintegration into ligaments and fragmentation into droplets. The work reported here is aimed at providing further insight into this effect on the fundamental hydrodynamics associated with liquid sheet development and drop formation.

The first set of experiments presented here consider the impact of two jets with a fixed angle of 90° and investigate, at a fundamental level, the parametric influence of the jets pre-impingement length and misalignment on the multijet impingement atomization process. The overall water flow rates are below 0.6l/min, corresponding to Reynolds numbers for each jet (Re_j) between 1400 and 5800. For this flow rate range, gravity effects have been found negligible. The pre-impingement distance normalized by the jet diameter (l_{pi}/d_j) ranges between 2.5 and 7.5, and experiments are performed for misalignments of 10, 30 and 50% of the jet diameter. The following section presents the experimental setup and the image processing algorithm used to obtain quantitative data of the

*Corresponding author: mpanao@dem.ist.utl.pt

liquid sheet characteristics and drop size. Afterwards, the results are presented and discussed in terms of the parametric effects of the pre-jet-impingement length and jet misalignment. Finally, before the concluding remarks, some considerations are made relatively to the relation between the transition of hydrodynamic regimes and the jet impact angle (2θ).

Experimental Methods

An experimental facility has been built to perform fundamental studies on multijet impingement atomization up to the simultaneous impact of 4 jets, although the experiments reported in this work consider only the impact of two jets. These are formed by two pipettes with 1mm of inner diameter (d_j), thus defining the jet diameter. The pipettes are assembled in a platform which allows their movement with 4 degrees of freedom (x, y, z, θ), thus, enabling variations of the jet pre-impingement distance (l_{pi}), as well as control the jet misalignment from their main central axis ($\delta_y = y/d_j$), as it is illustrated in Figure 1.

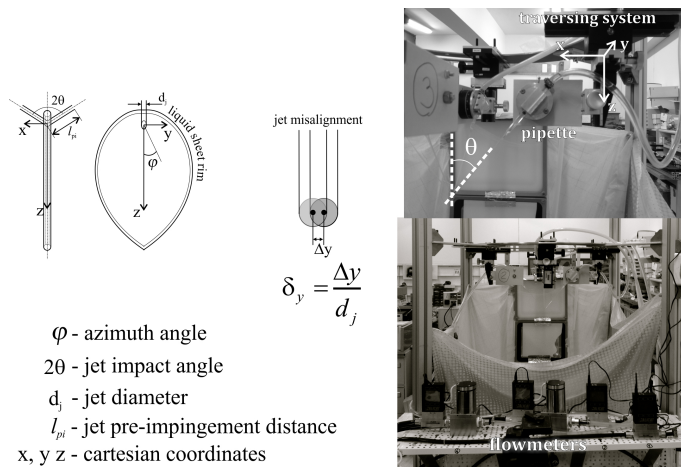


Figure 1. Parametric scheme of the two-impinging jets and jet misalignment (left); Photo of the experimental facility (right).

The experimental facility operates in a closed circuit, departing from a reservoir of water and distributing the overall volumetric flow rate by the pipettes. The flow rate in each pipette is controlled and measured by ALICAT LCR and L flowmeters, ranging up to a 2l/min, with a precision of the order of magnitude of 10^{-2} l/min. Finally, the reservoir is open at the top, thus, collecting the atomized fluid, as well as the excess water from the distributor.

The characterization of the atomization process is made with backlight scattering visualization, using a high-speed camera Phantom v.4.3. Images of the flow are acquired at a frame rate of 2250 FPS covering an area of 512×512 pixel², corresponding to a resolution of 0.2mm/pixel. For the characterization of the width and length of the liquid sheet, as well as the measurement of drop sizes, an image analysis algorithm has been developed in Matlab, with the following steps:

- Step 1. a first image is read and the user is asked to select the jet's limits, in order to obtain the resolution (mm/pixel), as well as the coordinates at the center of the jet impact point;
- Step 2. afterwards, for each image, the edges of the liquid structures are determined with the predefined Matlab *canny* method, which searches for the local maxima of the grayscale gradient calculated for the image using the derivative of a Gaussian filter. Using a threshold interval for the gradient values, the canny method allows that 'evident' edges are detected, as well as 'less evident' ones, in such way that the later must be related with the former. Thus, the edge identification procedure is less sensible to the noise in the image;
- Step 3. fulfill the areas which have a closed frontier and remove all elements with a morphology lower or equal to 2 pixel. The edge of potential droplets are detected in this step.
- Step 4. a droplet is validated if its sphericity is equal or greater than 90%;
- Step 5. finally, the length and width of the liquid sheet are measured with the jet impact center selected in the first step as reference point. The height from that point to the upper boundary of the liquid sheet is also

measured, since it is an important data for the design of multijet impingement atomizers.

At the end of these five general steps in the image processing, the following data are stored for further analysis:

$d_{d,i}$ a polidispersed sample of droplets size (d_d) per image i ;

L_i liquid sheet length from $\varphi = 0$ until $\varphi = \pi$;

$L_{ip,i}$ liquid sheet length from the jet impact point (ip) to $\varphi = \pi$

$W_{L,i}$ liquid sheet width

In this work, the first two datasets are considered in the analysis. An error propagation analysis applied to the measurement of the average drop size resulted in less than 1% and less than 1.5% relatively to the average length of the liquid sheet.

Results and Discussion

In the literature, two main flow regimes have been identified for the liquid sheet developed from the impact of two cylindrical liquid jets: the close-rim; and open-rim hydrodynamic regimes (see Fig. 2). While at relatively lower jet Reynolds number ($Re_j = u_j \cdot d_j / \nu$, where u_j is the jet velocity and ν the liquid kinematic viscosity), the liquid sheet rim closes at $\varphi = \pi$, for larger Re_j values, the liquid sheet disrupts at that location through Kelvin-Helmholtz instabilities [3].

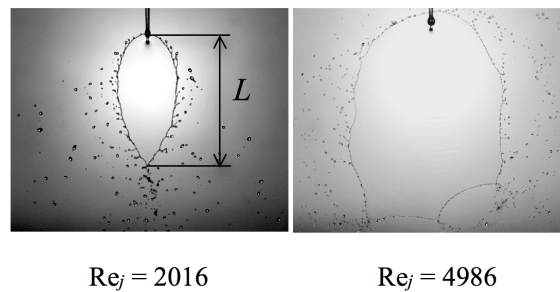


Figure 2. Examples of the close-rim (left) and open-rim (right) liquid sheet regimes for a normalized pre-impingement distance of $l_{pi}/d_j = 2.5$.

The results obtained in the image analysis of the flow are used to assess the parametric influence of the pre-impingement distance and jet misalignment of the liquid sheet morphology and drop size. Moreover, variations of the jet impact angle 2θ are also investigated relatively to the hydrodynamic regimes associated with the liquid sheet development.

Effect of pre-jet-impingement length on the liquid sheet characteristics

The results depicted in Fig. 3 correspond to the mean breakup length L , normalized by the jet diameter d_j , as a function of the jet Weber number $We_j = \rho u_j^2 d_j / \sigma$. The liquid properties ρ and σ correspond to the liquid density and surface tension, respectively, while u_j is the jet average velocity at nozzle exit. Up to $We_j = 100$, the hydrodynamic regime observed is the closed-rim, and above this value, the open-rim regime. While the pre-jet-impingement length l_{pi} does not apparently exert any effect on the breakup length, significant changes are observed in the open-rim regime. Namely, a substantial decrease of the breakup length L/d_j , with the attenuation of this effect for $l_{pi}/d_j > 6.8$.

The images in Fig. 4, for approximately the same Re_j range between 3183 and 3289 (or We_j between 140.5 and 150), allow observing the emergence of higher amplitude instabilities for $l_{pi}/d_j > 6.8$, as well as lateral breakups in the liquid sheet, justifying how - on average - its disintegration length becomes shorter.

In order to interpret these results, one should consider that a longer distance made by the free liquid jet before impaction with its opposite implies a greater relaxation of the velocity profile toward uniformity due to the absence of a non-slip condition. This suggests that altering the stress forces between the liquid and its surroundings [10] will influence the amplitude of the instabilities propagating from the jet impact location. In fact, Lin and Reitz [11] have argued that such relaxation process may amplify the natural instabilities inherent to the jet, which are likely to emerge from the sudden change of boundary condition (slip to non-slip). Once amplified, the propagation of

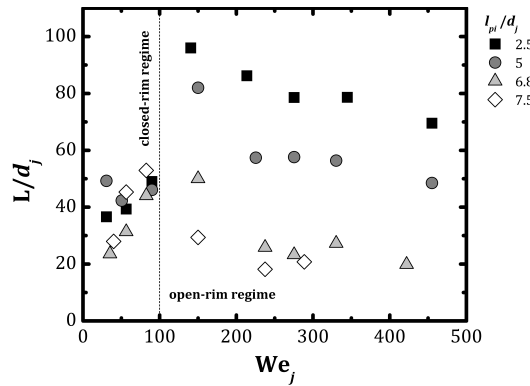


Figure 3. Effect of the pre-impingement distance l_{pi} on the liquid sheet disintegration length L/d_j .

these instabilities through the liquid sheet would promote its disintegration at shorter lengths, justifying the results depicted in Figures 3 and 4 in the open-rim hydrodynamic regime. The attenuation observed for $l_{pi}/d_j > 6.8$ also suggests the existence of an upper limit for this relaxation effect of the jet velocity profile over the liquid sheet's breakup length.

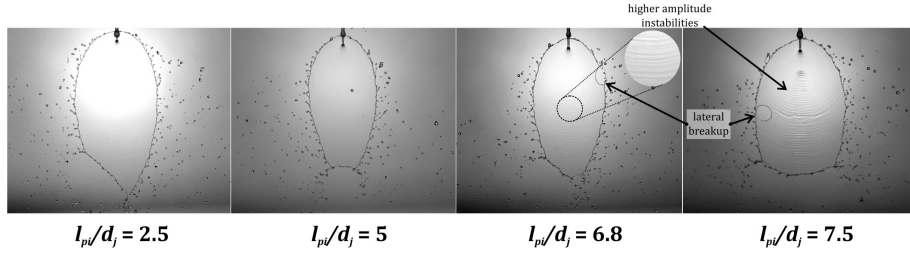


Figure 4. Visualization of the pre-impinging jet length on the liquid sheet development for $Re_j = 3183 - 3289$ or $We_j = 140.5 - 150$.

Effect of pre-impingement length on droplets characteristics

For each image, a drop size is measured according to the sphericity criterion, and the distribution of drop sizes is analyzed in terms of average values, as well as the average number of droplets identified per image. Generally, the number of droplets increases with the jet Reynolds number (Re_j). However, while in the closed-rim regime, the pre-jet-impingement distance l_{pi} does not produce any discernible effect over the number of validated drops (N_d), or their mean size, again, significant changes are observed in the open-rim regime. In this case, although with $l_{pi}/d_j = 2.5$, the number of droplets remains unaltered; for $l_{pi}/d_j > 2.5$, this number systematically increases with Re_j and l_{pi}/d_j . Such increase of N_d is followed by a decrease of their average size, as it would be expected by mass conservation, although differences are attenuated, once more, for $l_{pi}/d_j > 6.8$. The experimental results presented here suggest that increasing the jet distance from the impact location implies a spray with more and smaller droplets if the regime is the open-rim.

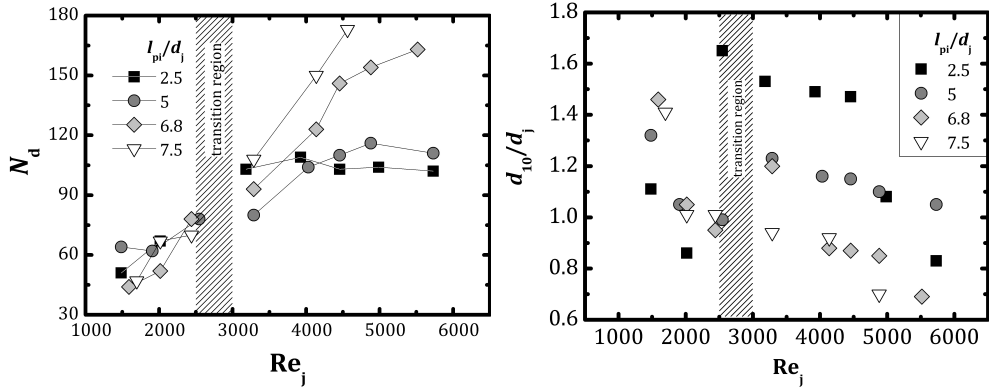


Figure 5. Effect of the pre-jet-impingement distance on the number of droplets per image (N_d - left), and their normalized mean size (d_{10}/d_j - right).

Effect of jet misalignment

The misalignments analyzed correspond to deviations $\delta_y = 10, 30$ and 50% of the jet diameter and the effect is observed in Fig. 6 for a low $Re_j = 2500$. The larger the jet misalignment, the longer is the length of the liquid sheet L/d_j , and the regime remains unaltered despite the higher instabilities observed at $\delta_y = 0.5$. By mass conservation, this enlargement of the liquid sheet implies, necessarily, a decrease of its thickness, thus, a greater proneness to the observed instabilities.

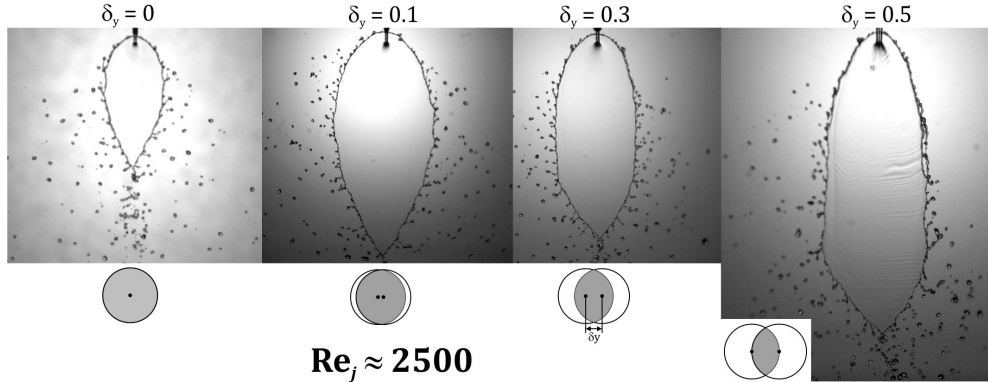


Figure 6. Images of the effect generated by jet misalignment on the length of the liquid sheet at $l_{pi}/d_j = 5$ for a condition in the closed-rim regime.

In the case of the open-rim regime, the jet misalignment effect suggested, i.e. promoting the liquid sheet enlargement along with the decrease of its thickness, is expressed by an early breakup of the liquid sheet, relatively to the $\delta_y = 0$ case. Namely, while this is more evident in the experimental movies made with the high-speed camera, for the larger misalignment ($\delta_y = 0.5$), the morphology of the atomization process is altered for this regime. This change leads to the emergence of a spray from the liquid sheet tip, as indicated in Fig. 7. Droplets formed by this mechanism have a larger diameter, leading to an overall increase of the mean drop size of the spray in these conditions.

If the Re_j range used in this work is considered, one observes in Fig. 8 (left) how the jet misalignment produces an increase of the liquid sheet in the closed-rim regime, practically independent of δ_y and, in the open-rim regime, for $Re_j > 4500$. Relatively to the mean drop diameter (Fig. 8-right), such misalignment leads to a systematic decrease of that value, except for $\delta_y = 0.5$, probably due to the emergence of larger droplets from instabilities in the closed-rim case, and from an atomization in the liquid sheet tip in the open-rim case.

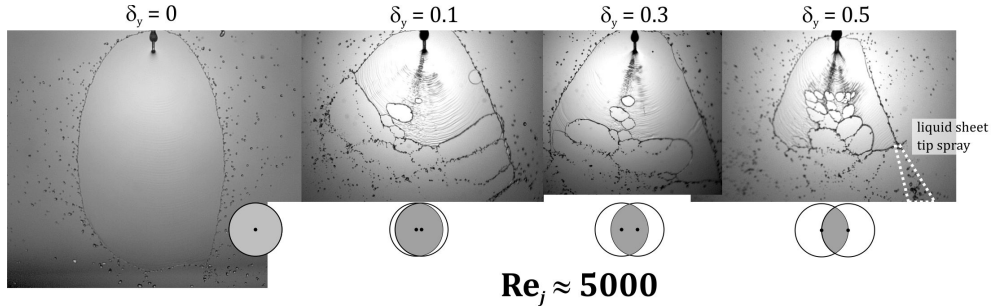


Figure 7. Images of the effect generated by jet misalignment on the length of the liquid sheet at $l_{pi}/d_j = 5$ for a condition in the open-rim regime.

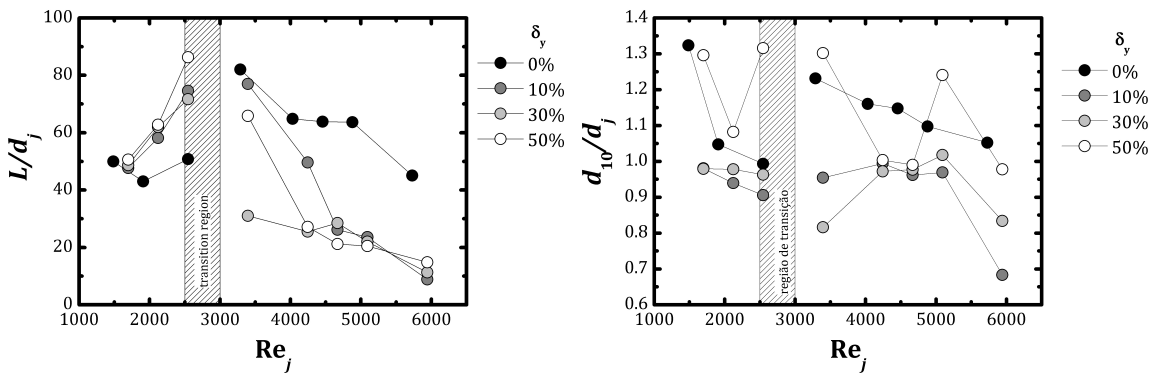


Figure 8. Effect of jet misalignment δ_y (in percentage) on the liquid sheet length (left) and mean drop size (right), both normalized by the jet diameter, as a function of the jet Reynolds number Re_j .

Some consideration on the effect of impact angle in transition from closed-rim to open-rim

The impact angle is a key parameter in the majority of multijet impingement sprays studies because it defines the liquid sheet shape and, consequently, its length. In this final section, the influence of the pre-impingement distance is compared with that exerted by changing the impact angle.

Fig. 9 shows that the impact angle variation has more influence in the liquid sheet length than l_{pi} . Namely, the normalized liquid sheet length increases significantly less or even decreases, as in the open-rim regime. This phenomenon is more evident for higher Reynolds. Another consideration is the shift of the transition region with Re_j . At lower Re_j , the transition between closed-rim and open-rim regimes occurs with $2\theta > 110^\circ$, while at higher Re_j , this transition occurs sooner at $2\theta > 80^\circ$. This challenges the results obtained by Li and Ashgriz [3], where the transition between these regimes does not seem to be significantly dependent on both 2θ and Re_j . Therefore, more fundamental research is needed to better understand this result.

Summary and Conclusions

In multijet impingement sprays, the atomization process consists in the formation of a liquid sheet developing from the jet impact location, which destabilizes in the rim, or in downward locations, to form ligaments. These further fragment into the droplets constituting the spray. According to the work reported in the literature, as well as the experimental evidence provided here, there are two regimes for the liquid sheet development, depending of the jet Reynolds number (Re_j). For lower $\text{Re}_j < 2500$, the rim bounding the liquid sheet closes in the entire azimuthal range (closed-rim regime), while for higher $\text{Re}_j > 3000$, the liquid sheet destabilizes downward in its interaction with the surrounding air (open-rim regime). The experimental results presented here evidence a transition between $\text{Re}_j = 2500$ and 3000 for $2\theta = 90^\circ$, however, it is also suggested that such transition may vary as a function of the impact angle as well.

In terms of the effect of the pre-jet-impingement length and jet misalignment, the analysis of the experimental results can be synthesized in the following:

- the pre-jet-impingement distance l_{pi} produces a significant influence on the liquid sheet breakup length in the open-rim regime, but not in the closed-rim.

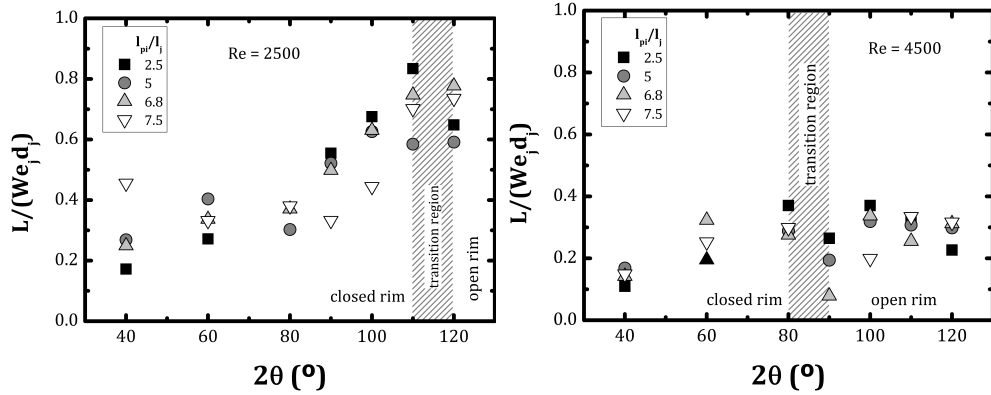


Figure 9. Evolution of the liquid sheet length, normalized by the Webber number and jet diameter, with the impact angle 2θ for $Re_j = 2500$ (left) and $Re_j = 4500$ (right).

- in the open-rim regime, higher impingement distances between the nozzle exit and the impact location (l_{pi}), result in shorter breakup lengths, smaller drop sizes, and more droplets. The interpretation suggested is related with the relaxation of the jet velocity profile which is higher for larger l_{pi} ;
- the misalignment of the jets induces a rotation of the liquid sheet, enlargement of its breakup length and, consequently, thinning of its thickness. In the case of open-rim regime, this amplifies the instabilities and anticipates breakup, decreasing its length;

Further studies will consider the fundamental hydrodynamics associated with multijet impingement sprays with more than two jets.

Acknowledgements

The authors would like to acknowledge Fundação para a Ciência e Tecnologia (FCT) for the financial support of this work through the project MUST (PTDC/EME-MFE/099040/2008). Miguel Oliveira Panão would also like to acknowledge FCT for supporting his research through fellowship (SFRH/BPD/45170/2008).

References

- [1] Panão, M.R.O, Guerreiro, J.P.P.V., Moreira, A.L.N., *International Journal of Heat and Mass Transfer*, 55, pp. 2854-2863 (2012)
- [2] Panão, M.R.O, Correia, A.M., Moreira, A.L.N., *Applied Thermal Engineering*, 37, pp. 293-301 (2012)
- [3] Li, R., Ashgriz, N. *Physics of Fluids* 18:087104 (2006)
- [4] Bremond, N., Villermaux, E., *Journal of Fluid Mechanics*, 549, pp. 273-306 (2006)
- [5] Shen, Y.-B., Poulikakos, D., *Journal of Fluids Engineering*, 120, pp. 482-487 (1998)
- [6] Choo, Y.J, Kang, B.S., *Physics of Fluids*, 19, 112101 (2007)
- [7] Anderson, W., Ryan, S., Santoro, R., *NASA Prop. Eng. Res.*, 2, pp. 69-74 (1993)
- [8] Jung, S., Hoath, S.D., Martin, G.D., Hutchings, I.M., *Physics of Fluids*, 22, 042101 (2010)
- [9] Gadgil, H. P., Raghunandan, B. N. *Atomization and Sprays* 19:1-18 (2009)
- [10] Lin, S. P., *Cambridge University Press* pp. 115-116 (2003)
- [11] Lin, S. P., Reitz, R. D., *Annual Reviews of Fluid Mechanics*, 30, pp. 85-105 (1998)